Shahrood University of Technology

Journal of Mining and Environment (JME)

Journal homepage: www.jme.shahroodut.ac.ir

Iranian Society of Mining Engineering (IRSME)

Modeling multi-phase reactive transport of petroleum hydrocarbons in Rey industrial area

Azadeh Agah[1]*, and Faramarz Doulati Ardejani[2]

1. Mining Engineering Department, Engineering Faculty, University of Sistan and Baluchestan, Zahedan, Iran
2. School of Mining, College of Engineering, University of Tehran, Iran

Article Info

Received 19 January 2024
Received in Revised form 25 May 2024
Accepted 30 October 2024
Published online 30 October 2024

DOI: 10.22044/jme.2024.14087.2624

Keywords

Two-dimensional model
Multi-phase reactive transport
Non-aqueous phase liquids
Groundwater
Rey industrial area

Abstract

This study aimed to develop a model to illustrate the migration of petroleum hydrocarbons that penetrate the underground environment due to leakage from storage tanks located below the surface.The transport model for non-aqueous phase liquids was integrated with contaminant transport models in two dimensions to forecast the contamination of groundwater and soil-gas resulting from the migration of light non-aqueous phase liquids on the water surface. The finite volume method was employed to obtain numerical solutions. The findings indicated that evaporation significantly influences the migration of non-aqueous phase liquids. The soluble plume's production and movement were impacted by the geological features of the location and the existence of the free phase plume. Comparing the model predictions and the results from the field studies for the thickness of non-aqueous phase liquids plume over water indicates a good agreement between the results of the two methods with an average error of less than 5%. The maximum thickness of non-aqueous phase liquids plume between 7 and 7.5 meters was obtained at a distance of 2250 meters from the beginning of the investigated profile. Although 36 years have passed since the leakage occurred, a significant amount of the spilled mass still remained in the non-aqueous phase liquids. The prolonged migration of non-aqueous phase liquids over this time period has led to the contamination of groundwater and the accumulation of significant quantities of contaminated soil.

1. Introduction

Petroleum hydrocarbons are extensively discharged into the environment due to human activities, as evidenced by studies conducted by a number of researchers [1-5]. At present, one of the environmental concerns is the pollution of aquatic environments by petroleum hydrocarbons. Organic compounds, hydrocarbons, and chlorinated solvents are widely produced and used around the world by various industries. As a result of accidental spills, incomplete disposal methods, and leaks from subsurface reservoir facilities, petroleum hydrocarbons enter the subsurface environments and ultimately contaminate valuable groundwater resources [6-10]. Soil and groundwater systems are commonly affected by petroleum hydrocarbons, which are the most prevalent pollutants found in these environments [11, 12] which are classified into light non-aqueous phase liquids (LNAPL) or dense non-aqueous phase liquids (DNAPL) based on their relative densities, respectively. After reaching the vadose zone, LNAPLs may be suspended in the residual phase or migrate upward through pores or downstream of groundwater [13-17]. LNAPLs often demonstrate mobility close to the groundwater table, while DNAPLs possess the capability to permeate saturated soils and travel to greater depths until they come across an impenetrable obstacle [18]. Both categories of NAPLs pose a potential hazard to the surrounding vicinity and the environment. When LNAPLs are trapped and separated by bubbles, it leads to an increase in the interfacial area of water, thereby enhancing the dissolution of LNAPLs [19,20].

* Corresponding author: agah_eng@eng.usb.ac.ir (A. Agah)

Once trapped within porous media, LNAPLs become long-term sources of contamination that gradually diminish over time [21]. An LNAPL free-phase pool facilitates soluble plume transport and significantly extends plume width [2, 3, 22, 23]. LNAPL migration is influenced by various thermodynamic fluid properties such as viscosity, density, surface tension, wetting, and variable chemical composition. Additionally, the properties of the porous rock environment, including grain size distribution, permeability, spatial heterogeneity, and moisture content, play a significant role [24]. In the vadose zone, the pore space of the rocky environment can be simultaneously occupied by water, gas, and LNAPL. This phenomenon, commonly known as multi-phase fluid flow [15], is crucial for comprehending the behavior of LNAPL migration beneath the surface. Understanding the transport of LNAPL through a porous medium involves the formation of a multiphase flow. The properties of NAPL, including density, viscosity, surface tension, solubility, and vapor pressure, play a crucial role in predicting subsurface contamination and comprehending NAPL transport, as stated by Rivett et al. [25].

LNAPL compounds can be categorized into either the soil-gas phase or groundwater prior to undergoing decomposition or biodegradation, based on their solubility and vapor pressure, without entering the aqueous phase [26-28]. The natural dilution of the source area depends on various factors, including the complexity of the LNAPL distribution beneath the surface, the segregation characteristics of LNAPL components, the physical properties of the environment, the fluid flow conditions, the types of microorganisms and their predators, the availability of electron and nutrient receptors, and environmental parameters like temperature and pH [29-34].The movement of LNAPLs in an unsaturated porous medium is complex enough when there are only two phases of liquid air and water. When the third fluid phase is involved like an immiscible organic liquid, the flow becomes more complex. The movement of LNAPLs in the subsurface is primarily influenced by mechanisms and hydrodynamics processes [35]. Dispersion and advection mechanisms play a significant role in influencing the movement and spread of contaminated plumes in a porous medium across a vast area. On the other hand, the absorption of soluble constituents leads to the separation of species between solid and aqueous phases, resulting in a decrease in pollutant mass within the solution. However, the uptake of pollutants is the primary cause of soil contamination within the soil phase. The subsurface microbial population's natural ability to biodegrade organic pollutants offers an effective means of pollutant removal from the aquifer, eliminating the need for physical extraction. The spatial distribution of LNAPLs in soil and water systems is influenced by various environmental factors, including temperature, soil moisture, nutrient supply, and fluctuations in water levels. Of these factors, water content is particularly important in determining the distribution of LNAPL plumes in aquifers.When water levels rise, the plume moves upward and increases the plume cover level. Water level fluctuations can cause LNAPLs to become trapped in soil pores.

The complex nature of these pollutants often causes improvement efforts to fail or be less effective than expected. Due to the importance of protecting groundwater resources, the use of low-cost and effective methods to accurately predict the contaminated area due to hydrocarbon spills is essential. Models can be a powerful tool for predicting the evolution and transport of pollutants, including petroleum hydrocarbons, in groundwater. Transport processes that can be more or less dominant in different stages of transformation of oil pollutant leakage in groundwater are broad-spectrum processes, dispersion, non-aqueous phase liquid (NAPL), surface adsorption to aquifers, and decomposition, biological [26-28]. Considering all these processes can be effective in the comprehensive assessment of the natural dilution of hydrocarbon compounds in groundwater or to design a suitable strategy for the treatment of groundwater aquifers from hydrocarbon compounds. To make more realistic and comprehensive modeling of the processes involved in the pollution of aquifers with petroleum hydrocarbons, sufficient data and a correct conceptual model that shows the effective mechanisms in contaminant transport, plume contamination development, as well as hydrogeochemical reactives are required [36-38]. In presenting a conceptual model, understanding the characteristics of the aquifer, geochemistry, determining the boundaries of the study area and the purpose of modeling is essential.

The evaluation of natural dilution and plume contamination can be achieved by integrating field data with numerical models that simulate reactive transport and biodegradation processes. These models can effectively summarize information collected in desert environments, quantify the balance of pollutants, dilution rates, and the

relative significance of concurrent processes. However, limitations in field sampling pose a challenge in accurately establishing mass balances for pollutants and determining the rate and quantity of removal through natural dilution, biodegradation, and adsorption. Utilizing a numerical model becomes possible when there is enough data, enabling the implementation of conceptual models, the quantification of effective processes in natural dilution, and the forecasting of plume evolution. Despite the efforts of researchers in developing various models, comprehensive and detailed modeling of natural dilution, hydrocarbon transport, and evolution is still impeded by computational limitations, inadequate field data, and insufficient understanding of field-scale processes. Hence, there is a need to develop more comprehensive models. Over the past few decades, a multitude of studies have been carried out to examine the movement of BTEX in the underground environment [39-47].

Several numerical models have been developed to investigate the penetration of VOC vapor and its concentration indoors [48-55]. The study of the degradation of NAPLs at the subsurface level is a subject of investigation in various environmental contexts. Instances of biodegradation and the natural reduction of contamination in groundwater aquifers serve as examples [56-68] and the penetration of volatile organic contaminations through the vadose zone in buildings [69-72].

The existence of soil and groundwater pollution in Rey industrial area has been evident since long ago. However, the source and extent of the contamination remain unclear. Considering the problem of water and soil pollution in the region, which is considered a serious risk for the residents around the refinery, this research can be a suitable basis for introducing a new and necessary technology to clarify the exact situation of oil pollution in soil and groundwater that has occurred so far. Numerical models have already been presented to predict the fate and transport of pollutants in the Rey industrial area, especially in the saturated zone of the aquifer system. These models are not able to fully describe all the aspects and complexities of the presence of oil pollutants in the aquifer system and provide a basis to develop an appropriate polluted water remediation method. Therefore, a more comprehensive model is needed that, in addition to the saturated zone of the aquifer, examines the distribution and transport of reactive pollutants in the unsaturated flow medium considering multiphase flow conditions. Hence, the objectives of this study were to model the multiphase reactive transport of petroleum hydrocarbons in the Rey industrial area and to study the effects of evaporation and dissolution on LNAPL transport. The study utilizes a two-dimensional model proposed by Kim and Kurapci Oglu to consider the presence of solution, soil-gas, and other remaining phases [73]. To conduct the modeling process, a finite volume model was developed by modifying a widely-used commercial software known as PHOENICS which was developed by CHAM Company, UK [74]. Adjustments for mathematical expressions pertaining to chemical and biological reactives were implemented through the creation of a PHOENICS input file and the inclusion of supplementary FORTRAN code within the GROUND subroutine [67, 75, 76]. The PHOENICS solver utilized these FORTRAN encodings exclusively for any non-standard computations throughout the solving procedure.

2. Geology and topography

Geologically, almost all parts of Tehran, including tuff, andesite, tufted andesite, and agglomerate belong to the Eocene period. The eastern part consists of Devonian period conglomerates and Mesozoic carbonate rocks. The southern part is covered with tuff and andesite from the Eocene period and is lower than sea evel [77]. The urban area of Tehran is located on alluviums resulting from extensive erosion of the Alborz Mountains (Figure 1).

The topographic situation in the urban area of Tehran consists of two parts: plain and mountainous areas. The northern parts of the urban area of Tehran are located in the mountainous region and as a part of the Alborz Mountain range with a length of 300 km from east to west, where all kinds of folded features can be seen. This area is covered by older alluvium but new alluvium is also found in part. The topography around Tehran Oil Refining Company shows that the height of the area decreases slowly from north to south and is difficult to slope in the east to west direction. The topography of Tehran Oil Refining Company fluctuates in the range of fewer than 7 meters and its average altitude is approximately 1030 meters above sea level. There are two faults in Rey industrial zone, including Tehran Oil Refining Company. One of them is located near Azimabad, which extends to Shahrehabad in the west. But this fault is old and it is full of clay, sludge, and alluvial sediments.

In the southern part of Rey district, south of Qala-e-Naw, a fault with a length of 18.5 km extends from east to west. This fault is also old and its activity has stopped [77].

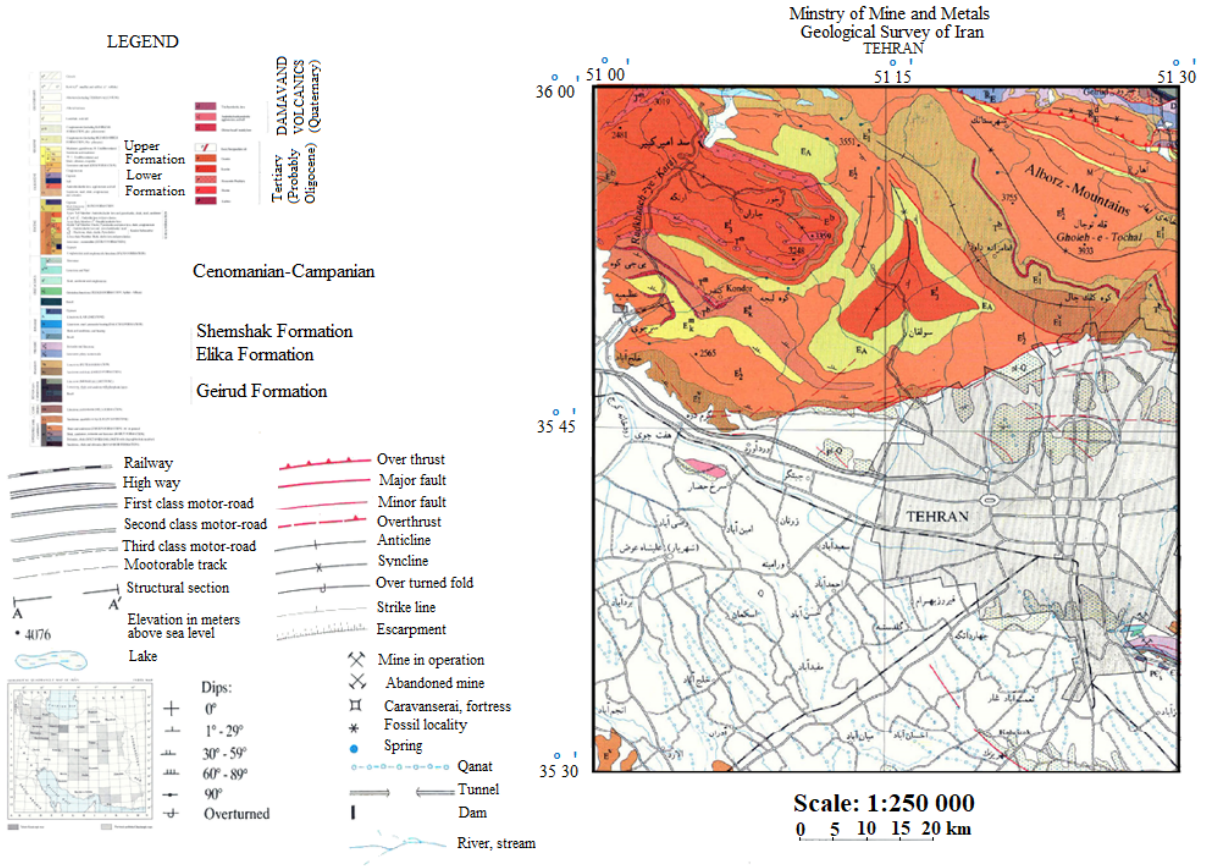

Figure 1. Geological map of the study area [77].

2.1. Geological structure

The geological features of REY industrial area were recognized up to the depth of 40 m by considering the results of geological strata obtained from core observations.

The stratum of investigation area were found to contain 3 layers, up to the depth of 40 m.

1) Geological profile map of REY industrial area

Based on the observation results of each bore, the geological profile of REY industrial area was drawn up. Figure 2. shows the positions that were used for preparation of this geological profile map.

2) Geological structure of REY industrial area

Figure 3 and Figure 4 show the geological profile maps. Regarding the drawn map in which the ratio of horizontal direction/Vertical direction was 1:40, it was emphasized in the vertical direction.

The following points can be considered on the geological characteristics of REY industrial area:

- On the basis of core observation, ground layers configuration of REY industrial area has been classified of 3 layers: a layer of gravel, one layer of sand and another layer of clay.
- The ground configuration of REY industrial area includes a stratum with thickness of 10 m consisting of clay and a stratum with thickness of 1～10 m consisting of silt which are not the main part and fine sediment of them is the dominant part.
- Although gravel bed with a thickness of several ten centimeters has been sandwiched but it is concluded that the layer is thin and has a local distribution.
- Only in the position of CB1, sand stratum and gravel stratum (S1, G1 layer) was verified and it is concluded that the distribution is local.
- Generally, the distribution of stratum is horizontally parallel to the topographic structure of ground.

- The whole region of REY industrial area is almost uniform consisting of clay and silt ground.
- The stratum is not recognized as permeable layer.
- There was no certain impermeable layer like an existing artesian groundwater.

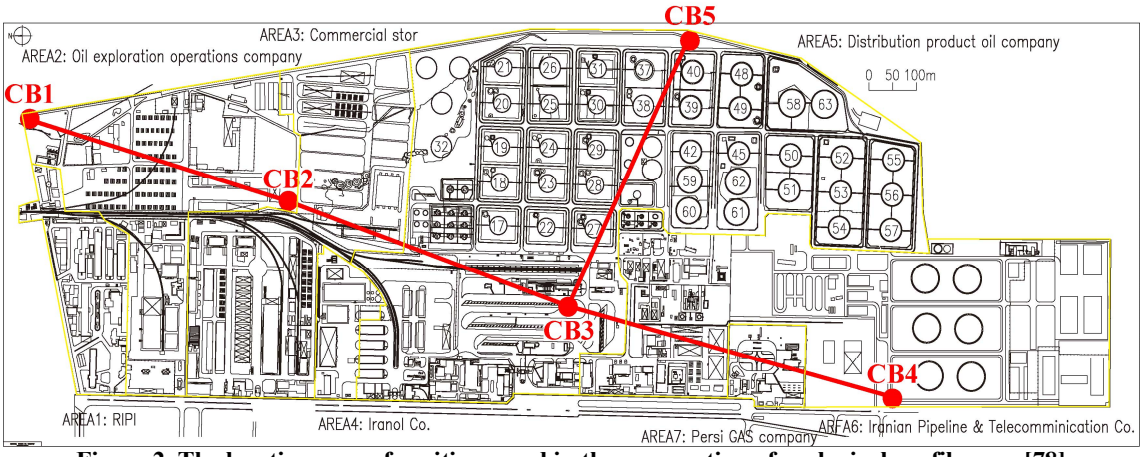

Figure 2. The location map of positions used in the preparation of geological profile map [78]

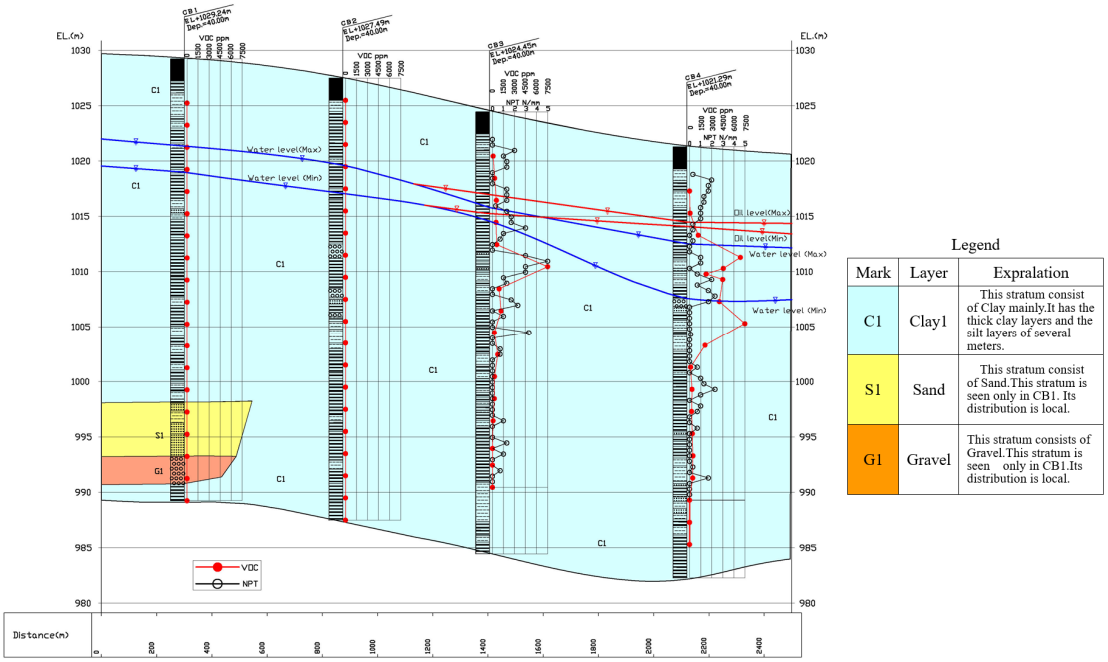

Figure 3. Geological profile of CB1~CB4 [78].

3) Stratum of the ground in REY industrial area

In the investigation area, the ground is mostly consisting of clay with a uniform characteristic.

The configuration of stratum distribution in the ground of REY industrial area obtained within the depth of 40 m is explained as follows. Stratigraphical chart of ground in the REY industrial area is shown in Table 1.

- Clay stratum 1 (C1 layer)

It consists of a different kind of gravel that is a mixture of clay and gravel. The ratio of gravel differs depending on the place, however, there is a semi-consolidate sand stone of gravel with a thickness of 1～2 cm.

In this stratum, one layer of sand with a thickness of 10 cm is pinched between gravel layer; however, it is concluded that without continuity it has been distributed locally.

C1 layer has been distributed in the whole investigation area with a thickness of more than 40 m.

- Sand stratum (S1 layer)

It consists of silt ~ fine sand ~ coarse sand.

Only the depths of 31~36 m in CB1 was verified. Distribution at investigation area is limited around CB1. There is a possibility of continuity in the northern side of investigation area.

Thickness is approximately 5 m.

- Gravel layer (G1 layer)

It mainly consists of fine gravel and coarse sand.

Only the depths of 36~39 m in CB1 was verified. Distribution at investigation area is limited around CB1. There is a possibility of continuity in the northern side of investigation area.

Thickness is approximately 3 m.

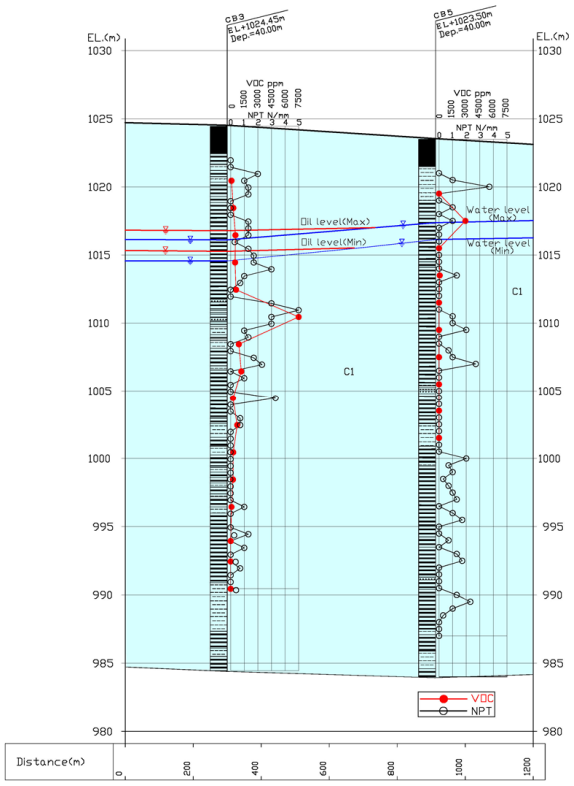

Legend

Mark	Layer	Expralation
C1	Clay1	This stratum consist of Clay mainly.It has the thick clay layers and the silt layers of several meters.
S1	Sand	This stratum consist of Sand.This stratum is seen only in CB1. Its distribution is local.
G1	Gravel	This stratum consists of Gravel.This stratum is seen only in CB1.Its distribution is local.

Figure 4. Geological profile of CB3~CB5 [78].

Table 1. Stratigraphical chart of ground in the REY industrial area [78].

Stratigraphic name	Thickness of stratum (m)	Composition	Distribution
Clay stratum 1	More than 40 m	Clay, silt (sand, gravel)	Whole area of investigation
Sand stratum	About 5 m	Silt ~ Coarse sand	From near of CB1 to north side
Gravel stratum	About 3 m	Fine gravel ~ coarse sand	From near of CB1 to north side

3. Materials and Methods

3.1. Transport equation of LNAPL through the groundwater table

Within the NAPL region, which consists of mobile LNAPL, there exists residual saturated water, mobile NAPL, and three solid phases. The aqueous phase is regarded as the wetting phase, while the NAPL phase is considered the non-wetting phase. The premise suggests that the solid phase is submerged in water, and there is no physical interaction between NAPL and the the solid phases. It is assumed that there is a local equilibrium between the phases, and the transfer of mass from the NAPL zone to the vadose zone (via evaporation) and the saturated zone (via dissolution) is considered. In terms of the thickness of the NAPL lens and other averaged parameters, the governing equation that describes transportate of NAPL on the water table can be formulated as follows [73]:

$$\frac{\partial L}{\partial t}+\frac{q_w K_o}{K_w n S_{oo}}\nabla L-\frac{K_o L_o(\rho_w-\rho_o)}{n S_{oo}\rho_w}\nabla^2 L=\pm\frac{Q_o}{n S_{oo}}\delta(x-\xi)(y-\zeta)+\frac{S_{oun}}{S_{oo}}\frac{\partial L}{\partial t}-\frac{E_N^g}{\rho_o n S_{oo}}-\frac{E_N^w}{\rho_o n S_{oo}} \quad (1)$$

where:

L: The thickness of the free product on the groundwater-surface (m);
L_o: NAPL lens reference thickness (volume per unit area of NAPL, divided by porosity filled with NAPL) (m);
n: porosity;
S_{oo}: Saturation degree of NAPL within the NAPL lens;
S_{oun}: Saturation degree of NAPL in the vadose zone;
K_o: NAPL hydraulic conductivity in NAPL lens (m/day);
K_w: Hydraulic conductivity of groundwater (m/day);
q_w: Special drainage of groundwater (m/day);
ρ_w: Water density;
Q_o: The Dirac delta function (δ) indicates the leakage/pumping rate of NAPL at the point (ξ,ζ), with a positive sign denoting leakage (m^3/day);
E_N^g: Mass transfer from NAPL phase to soil-gas due to the process of evaporation;
E_N^w: Mass transfer from the NAPL phase to groundwater due to dissolution.

3.2. Transport equation of dissolved contaminants in groundwater

In the saturated zone, water completely occupies the pore space, distinguishing it from other zones. It connects with the vadose zone through volatilization or dissolution and with the NAPL zone through dissolution. The behavior of contaminants in the saturated zone is influenced by chemical and biological transformation processes, as well as partitioning, resulting in their incorporation into a continuous mobile phase.The equation governing the transport of groundwater-soluble pollutants is as follows [73]:

$$b\frac{\partial}{\partial t}[nRC_w]+\nabla\cdot[bq_w C_w-bD\nabla(nC_w)]=-bR_{w,bio}+E_N^w-E_w^g \quad (2)$$

$$R=1+\frac{k_d\rho_b}{\theta} \quad (3)$$

$$E_N^w=-\theta_w D_D\frac{(C_w-C_w^s)}{l_c} \quad (4)$$

$$E_w^g=-\theta_w D_D\frac{\left(\frac{C_g-C_w}{H}\right)}{l_c} \quad (5)$$

where:

b: The depth of the aquifer measured from the groundwater level to the impermeable floor layer (m);
R: Linear absorption;
θ_w: water content;
$R_{w,bio}$: Biodegradation in the saturated area;
E_w^g: Soil-gas mass influx from groundwater;
k_d: Is the distribution coefficient that depends on the characteristics of the dissolved body and the solid environment (ml/g);
ρ_b: density of dry soil block (kg/m^3);
l_c: the thickness of the capillary margin (m).

The following model, which is a generalized Monod kinetics and was first proposed by Han and Levenspiel [79], has been used to simulate the degradation of the active component at low concentrations and the inhibition of the active component at high concentrations [80]:

$$\mu=\frac{\mu_{max}\left(1-\frac{C}{C_m}\right)^n}{C+K_S+\left(1-\frac{C}{C_m}\right)^m} \quad (6)$$

where:

C: Aqueous phase concentration of the compound (mg/l);
K_S: Constant (mg/l);
μ_{max}: Maximum special consumption rate (s^{-1});
μ: Special consumption rate (s^{-1});
C_m: The critical concentration is the inhibitor, in exchange for greater amounts of which the decomposition reactive stops (mg/l);
m and n: the coefficients are constant.

To illustrate, hydrocarbon compounds such as benzene, toluene, ethylbenzene, and xylenes are classified as toxic compounds. Even in concentrations below their solubility limit, they can cause the death of microbial cells [81]. Consequently, when a significant amount of these compounds are present, such as in a non-aqueous phase liquid like pure solvent or diesel in contact with water, there is a high likelihood of complete inhibition of microbial activity. This inhibition can lead to the prevention of biological degradation of the inhibiting compound.

3.3. Transport equation of a volatile contaminant within the vadose zone

The region located above the water table, where the NAPL is absent, is known as the vadose zone.

This zone comprises of water, soil gas, and solid components, and it is influenced by the the atmosphere, the saturated zone, and NAPL zone. In the event that the vadose zone gets contaminated by pollutants that have evaporated from saturated zone or the NAPL, it is presumed that these pollutants will evenly distribute among the different phases in a state of equilibrium. By applying the principle of mass conservation, the transport model for contaminants that have become volatilized in the vadose zone is established in relation to gas-phase concentrations, as outlined by Kim and Corapcioglu [73]:

$$d\frac{\partial}{\partial t}\left[R_g\theta_g C_g\right]+\nabla\cdot\left[dq_g C_g-d\left(D_g+D_{wr}H\frac{\theta_{wr}}{\theta_a}\right)\theta_g\nabla C_g\right]=-dR_{g,bio}+E_N^g-E_g^A+E_w^g \quad (7)$$

$$R_g=1+H\frac{\theta_w}{\theta_g}+k_dH\frac{\rho_b}{\theta_g} \quad (8)$$

$$D_g=\frac{\theta_g^{\frac{7}{3}}}{n^2}D_g^b \quad (9)$$

$$D_{wr}=\frac{\theta_{wr}^{\frac{7}{3}}}{n^2}D_w^b \quad (10)$$

$$R_{g,bio}=\lambda H\theta_w\left(1+k_d\frac{\rho_b}{\theta_w}\right)C_g \quad (11)$$

where:

q_g: Volumetric flux of soil-gas (m/day);
θ_w: Volumetric water content in the NAPL zone;
θ_g: Volumetric content of soil-gas;
D_g: Effective penetration coefficient of pollutants in soil-gas (cm^2/s);
D_{wr}: The coefficient for the successful infiltration of contaminants in the water present in an unsaturated region (cm^2/s);
D_g^b: Pollutant penetration coefficient in block air (cm^2/s);
D_w^b: Contaminant penetration coefficient in block water (cm^2/s);
$R_{g,bio}$: The vadose zone experiences general consumption through biodegradation in its solid, water, and gas phases;
E_g^A: The rate of transfer of mass from the vadose zone to the atmosphere.

For an impenetrable land surface, in Equation (7), E_g^A is equal to zero. To evaluate the mass flux into the atmosphere in the absence of pollution in the vadose zone, Equation (7) is not applicable for permeable ground. Conversely, the depth of penetration is regarded as the depth of the vadose zone. Equation (12) is utilized to calculate the transfer of mass from the NAPL phase to the atmosphere via the vadose zone [73]:

$$E_N^A=\left(\theta_g D_g+\theta_{wr}D_{wr}H\right)\frac{(C_G^S-C_A)}{d} \quad (12)$$

where:

D_g: Effective penetration coefficient of pollutants in the gas phase (cm^2/s);
D_{wr}: Effective penetration coefficient of the pollutant in the liquid phase of the vadose zone (cm^2/s);
C_A: Concentration of pollutants in the atmosphere (mg/l);
C_G^S: The pollutants in equilibrium with the vapor phase are saturated in the vapor phase (mg/l);
d: Depth of unsaturated area (m).

The PHOENICS software from the CFD package was utilized to solve the governing equations that depict LNAPL migration. PHOENICS is a versatile CFD package that has the capability to simulate fluid flow, heat transport, and mass transport [74]. However, Equations 1, 2, and 5 have certain terms that are not incorporated in the general PHOENICS equation, hence, necessitating the introduction of appropriate settings for each expression in PHOENICS.Q1 file and use of additional FORTRAN 99 programming under GROUND routine [75]. Figure 5 shows the main steps for a CFD analysis.

4. Set model and input data

A two-dimensional model was designed to simulate the multi-phase reactive transport of petroleum hydrocarbons in the Rey Industrial Zone. Because a variety of petroleum contaminants are identified in the groundwater aquifer in the area, the total amount of hydrocarbons is considered in the modeling. The simulation was performed on a cross-section similar to the geological profile *CB1-CB4* of Rey Industrial Zone (Figure 6).

The cross-sectional area in question spans 4000 meters horizontally and 36.5-49.7 meters vertically, encompassing a total of 2560 control volumes (Figures 6 and 7).

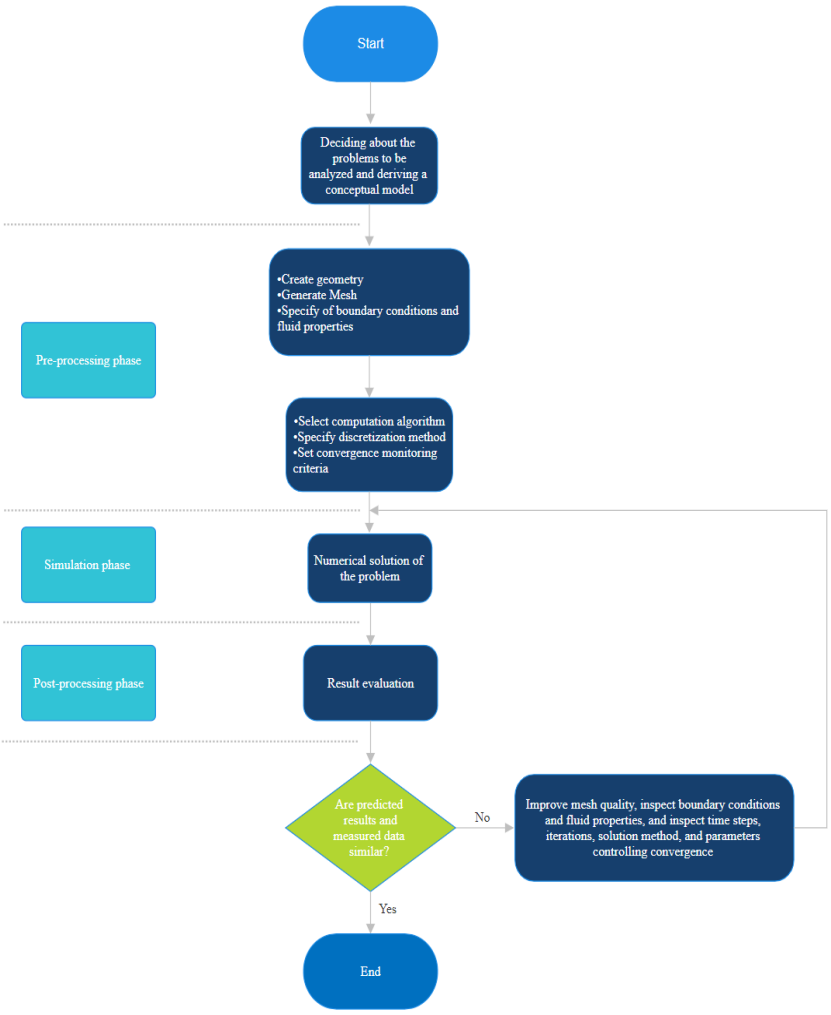

Figure 5. Main stages in a CFD simulation.

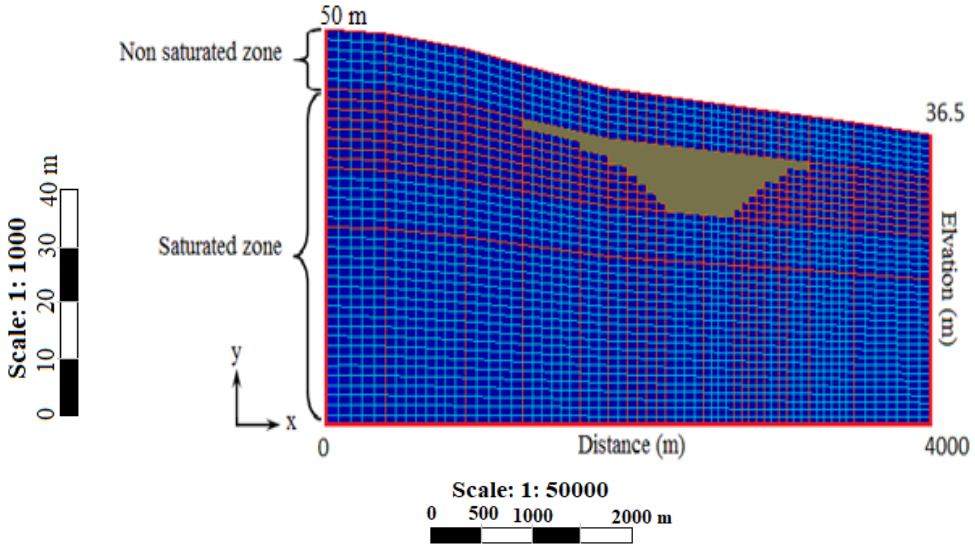

Figure 6. Two-dimensional cross-section: finite volume network (vertical axis is 40 times the horizontal axis).

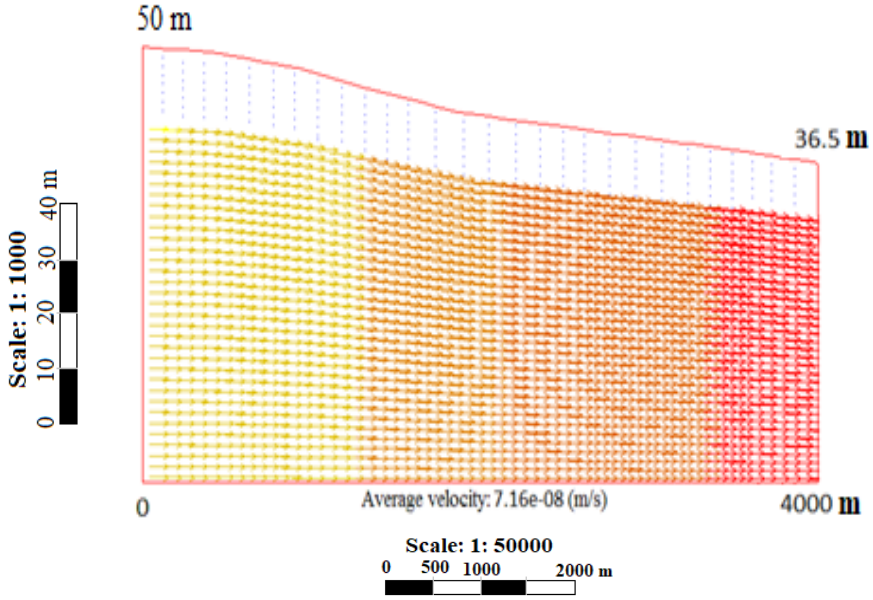

Figure 7. Velocity vectors of flow field.

The groundwater flow system was assumed to be steady-state. The difference between the hydraulic head between the left and right borders of the model is 10 meters. The average rainfall (feeding) was 0.25 m per year for the upper limit.

For simplicity in the modeling process, the horizontal velocity component in the unsaturated region was ignored and the vertical flow direction was assumed. Concentration values are presented in milligrams per liter. The model input data are given in Table (2).

5. Two-dimensional simulation results

5.1. Scenario 1: Two-dimensional modeling of LNAPL lens thickness on groundwater-surface

In the first step, to calibrate the model, the thickness of the LNAPL lens was simulated using Equation (1) presented in the second chapter. The simulation assumed the absence of direct contact between the solid phases and LNAPL, while also considering a state of local equilibrium between the phases.

The dissolution process facilitates the mass transport from the LNAPL region to the saturated region, while evaporation leads to its transfer towards the unsaturated region. The model was developed based on these assumptions and the results of the modeling, which were compared with field data, are presented in Figure (8). The time step for the comparison was 36 years. Figure (9) presents a comparison between the results obtained from numerical simulation and those derived from field studies. This comparison shows that the presented numerical model is well able to simulate the thickness of LNAPL plume on water.

5.2. Scenario 2: Two-dimensional modeling of the reactive transport of groundwater soluble hydrocarbons

In this scenario, the reactive transport of groundwater soluble hydrocarbons was modeled using Equation (2) presented in the second chapter. The dissolution of the NAPL region and the evaporation of the unsaturation zone are interdependent and influenced by the hydrocarbon concentrations in each respective region. In Equation (2), the term biodegradation of hydrocarbons is not considered and their chemical decomposition by first-order kinetics is considered in the model. In this scenario, the biodegradation model proposed by Han and Levenspiel (1988) (Equation 4) was used to model biodegradation [79]. Due to the toxicity of most petroleum hydrocarbons and their ability to kill microbial cells at concentrations below their potential, the presence of a significant amount of these contaminants in water can lead to the complete inhibition of microbial activity and the subsequent biodegradation of inhibitory compounds [81]. In this model, the critical concentration above which the biodegradation stops is considered to be 400 mg/L. The model was performed once with biodegradation and again without biodegradation. The simulation results at time intervals of 36 and 50 years are shown in Figures (10) to (13).

As can be seen in the above figures, the model is not significantly sensitive in terms of

biodegradation kinetics and the results obtained in the two cases are almost similar. This is because the concentration of soluble hydrocarbon contaminants is higher than the critical concentration and biodegradation practically does not occur due to the death of the microbial population at high concentrations.

Table 2. Input parameters used in the two-dimensional simulation.

Parameter	Value
Model length along x	4000 meters
Model width along y	36.5-49.7 meters
Number of volumetric elements	2560
Simulation time	50 years
Number of time steps	50
The number of repetitions	1000
Hydraulic conductivity of water along x	$8.07 \times 10^{-6}\, m/s$
Hydraulic conductivity of water along y	$8.07 \times 10^{-7}\, m/s$
Hydraulic conductivity of oil along x	$1.19 \times 10^{-8}\, m/s$
Hydraulic conductivity of oil along y	$1.19 \times 10^{-9}\, m/s$
Porosity (n)	0.41
Water content (θ_W)	0.2
Aired porosity (θ_g)	0.07
Porosity filled with oil (θ_{NAPL})	0.14
Fixed head on the left border	42
Fixed head on the right border	32
Longitudinal scattering coefficient (α_L)	15 meters
Transverse scattering coefficient (α_T)	1 meter
Water density (ρ_W)	$1000\, \frac{kg}{m^3}$
Oil density (ρ_{NAPL})	$800\, \frac{kg}{m^3}$
The saturation of non-aqueous phase liquid (NAPL) in the NAPL lens(S_{oo})	0.85
The residual saturation of water (S_{ow})	0.15
The residual saturation of NAPL (S_{oun})	0.05
Flow rate of the source of NAPL (Q_o)	$0.022\, \frac{m^3}{day}$
Delay factor (Q_o)	2
Petroleum hydrocarbon decomposition coefficient (k_1)	$0.00005\, \frac{1}{day}$
The thickness of the saturated area of the tablecloth (b)	28 meters
The thickness of unsaturated area (d)	12 meters
Capillary margin thickness (l_c)	0.07 meters
Pumping rate NAPL	$3\, \frac{m^3}{h}$

Because the groundwater flow rate is very low, the soluble phase plume is spread only in the free phase zone of the hydrocarbon pollutant. This is an advantage for the region in terms of designing cleaning methods. As can be seen, even after 50 years, the solution phase plume has a slight expansion in the direction of groundwater flow, so it can not cause contamination of adjacent areas.

5.3. Scenario 3: Two-dimensional modeling of the reactive transport of soluble hydrocarbons by considering the reduction of the free phase thickness on the groundwater-surface by pumping it

After completing field studies and measurements in 2007, as the first step to eliminating pollutants and cleaning the aquifer contaminated with oil, the free phase of pumping of these pollutants from the aquifer to the ground began took. However, despite the pumping operation in the area, due to the leakage from the upper layers of contaminated soil, a thin layer of free phase remains on the groundwater surface. The simulation results, in this case, show that although most of the free phase has been removed from the aquifer, the presence of this thin layer has caused the persistence of groundwater pollution on a significant scale (Figure 14).

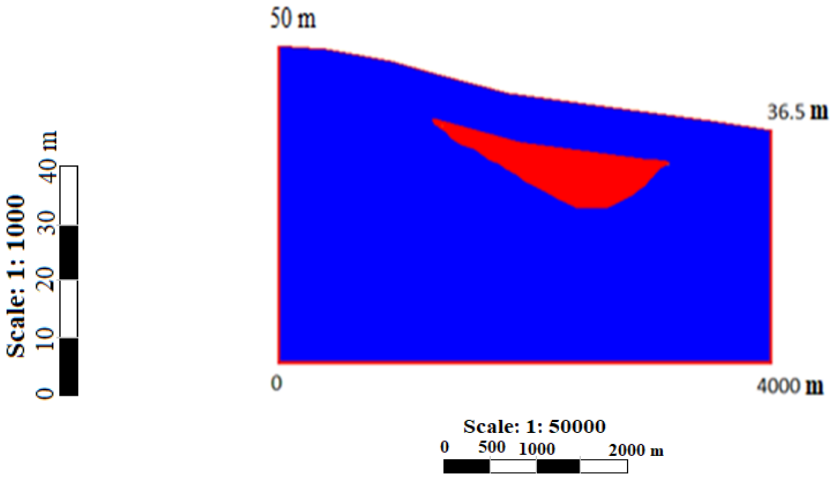

Figure 8. Two-dimensional simulation results: LNAPL lens thickness over 36 years.

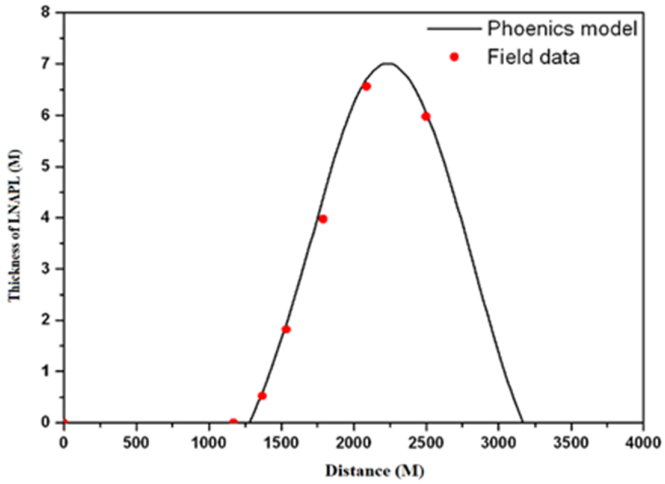

Figure 9. Comparison of the results obtained from the finite volume model with field data after 36 years.

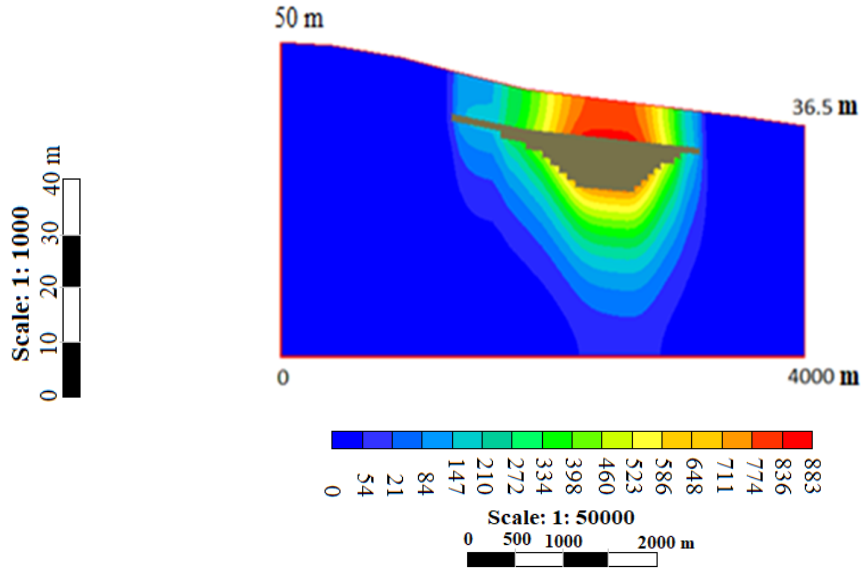

Figure 10. Two-dimensional simulation results: Distribution of soluble phase concentration (mg/l) for 36 years without considering biodegradation.

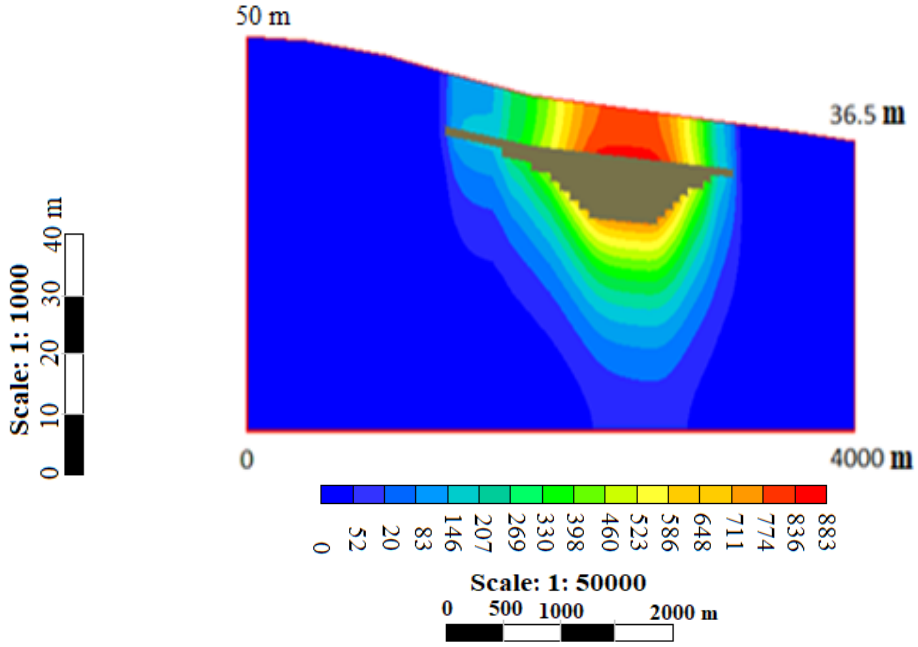

Figure 11. Two-dimensional simulation results: Distribution of soluble phase concentration (mg/l) for 36 years, considering biodegradation.

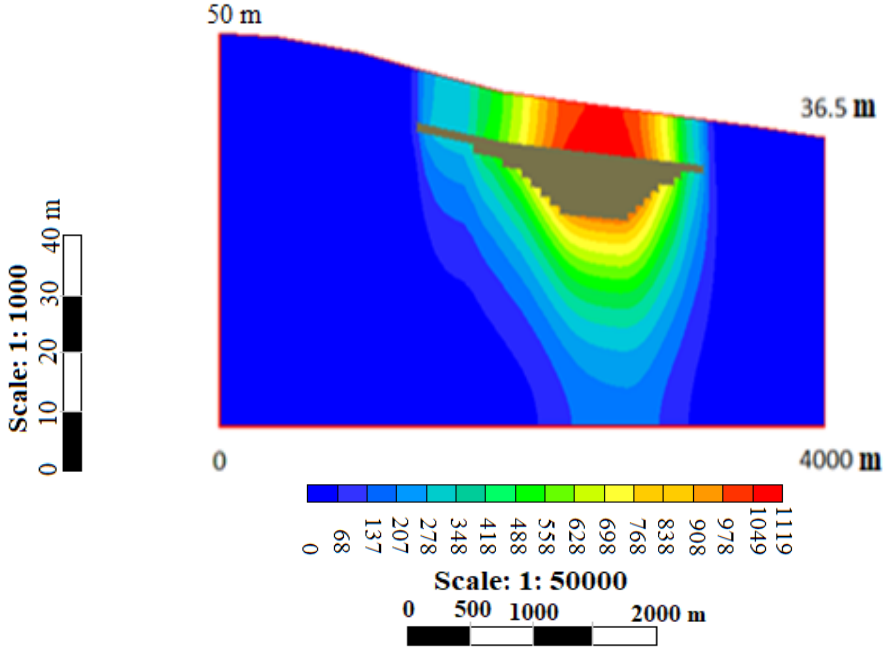

Figure 12. Two-dimensional simulation results: Distribution of soluble phase concentration (mg/l) for 50 years without considering biodegradation.

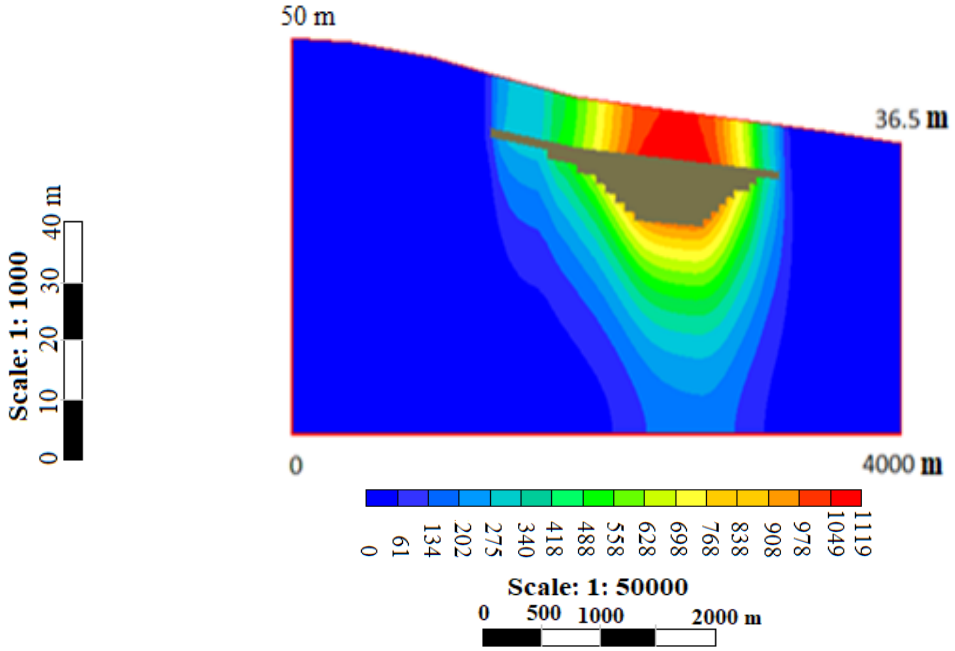

Figure 13. Two-dimensional simulation results: Distribution of soluble phase concentration (mg/l) for 50 years, considering biodegradation.

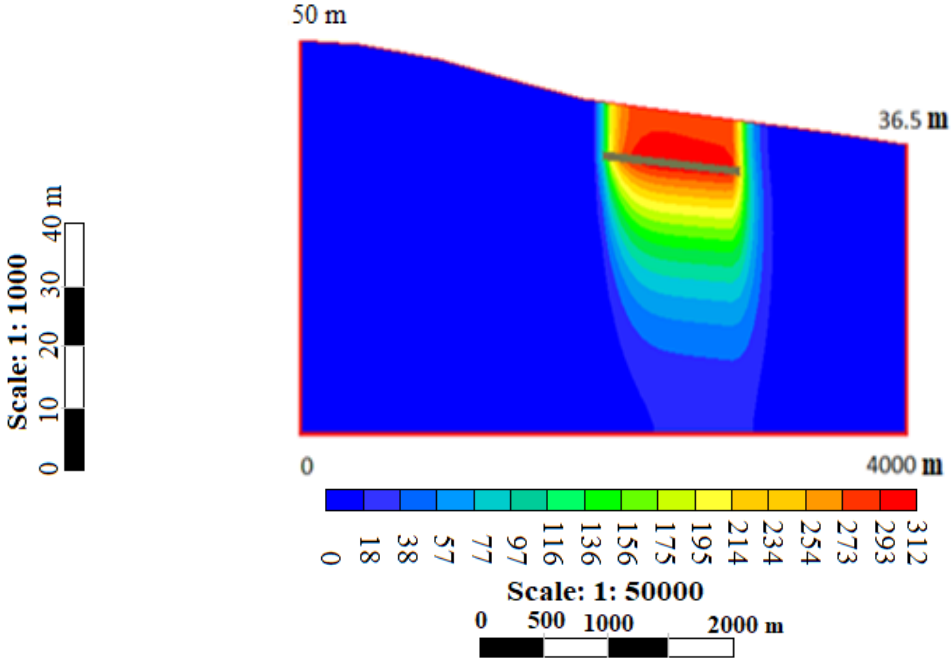

Figure 14. Two-dimensional simulation results: Distribution of soluble phase concentration (mg/l) for 50 years, considering biodegradation. In this scenario, a thin layer of the free phase of hydrocarbon pollutants remains on the surface of the groundwater aquifer after 50 years.

5.4. Scenario 4: Two-dimensional modeling of the reactive transport of groundwater soluble hydrocarbons considering that the free phase plume on the water is eliminated after 42 years

The fourth scenario is similar to the third scenario, except that in this case, it is assumed that due to the pumping operation after 6 years, the free phase is completely removed from the surface of the groundwater aquifer, and in this case, the model is implemented. The concentration distribution of the solution phase after 50 years is shown in Figure (15). This figure shows significant changes in the phase concentration distribution of petroleum

hydrocarbons, resulting in the elimination of the free phase after 42 years. However, the groundwater aquifer is still contaminated, and to clean the solution phase of the contamination, an appropriate and cost-effective remediation method, such as a biological remediation method, should be designed according to the conditions of the area.

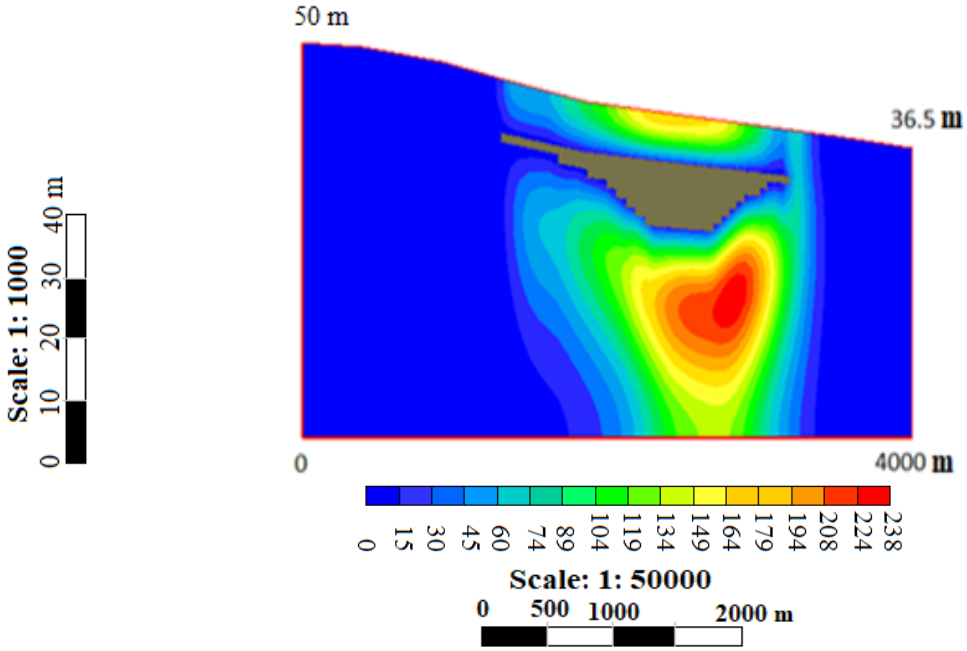

Figure 15. Two-dimensional simulation results: Distribution of soluble phase concentration (mg/l) for 50 years, considering biodegradation. In this scenario, the free phase of hydrocarbon pollutants was completely removed from the surface of the groundwater aquifer after 42 years.

5.5. Scenario 5: Two-dimensional modeling of the reactive transport of evaporated hydrocarbons in the vadose zone

Assuming the absence of NAPL phase in the unsaturated region, which comprises soil, water, and solid-gas phases, interactions with the NAPL region, saturation zone, and atmosphere are expected. If the unsaturated or saturated zone becomes contaminated with NAPL-evaporating contaminants, the distribution of pollutants between the phases is assumed to reach a local equilibrium. The two-dimensional modeling of petroleum hydrocarbon transport in this area relies on Equation (2-6). Figures (16) and (17) depict the simulation outcomes for time steps of 36 and 50 years, respectively.

Figure 19 shows that for 36 years, a significant amount of petroleum hydrocarbons have evaporated from the groundwater-surface as well as the free phase of NAPL and been transportred to the vadose zone. This indicates that the potential for volatile hydrocarbon pollutants in the area is high. However, Figure (17), which shows the distribution of gas-phase concentrations of petroleum hydrocarbons after 50 years, shows that the values of concentrations have decreased compared to the values shown in Figure (16). The extensive drilling conducted in the area for field studies between 2005 and 2007 has resulted in a decrease in hydrocarbon gas-phase concentrations in the unsaturated area. The decline in levels can be ascribed to the emission of a significant amount of gaseous substances, which were previously confined underground, into the atmosphere during the excavation process. Consequently, the accumulation of volatile hydrocarbons under the surface of the earth has been significantly reduced. Therefore, there has been a substantial reduction in the gathering of volatile hydrocarbons beneath the Earth's crust.

5.6. Scenario 6: The reactive transport of evaporated hydrocarbons in the vadose zone can be effectively modeled by incorporating the reduction of the free phase thickness on the groundwater-surface through pumping

This scenario is similar to the third scenario. It is assumed that as a result of the pumping operation after 2007 most of the free phase on the water surface has been eliminated and only a thin layer of

NAPL remains. The model was implemented with these conditions. Figure (18) shows the simulation result for a time step of 50 years. The comparison of Figures (17) and (18) shows that the removal of the free phase from the water surface plays an important role in reducing the gas phase concentration of volatile hydrocarbons.

5.7. Scenario 7: Two-dimensional modeling of the reactive transport of volatile hydrocarbons in the vadose zone, assuming that the free-phase plume on the water is eliminated after 42 years

In this scenario, it is assumed that the free phase plume on the surface of the groundwater disappears completely after 42 years. The result of this simulation for a time step of 50 years is shown in Figure (19). As can be seen in this figure, most of the gaseous phase of volatile hydrocarbons is transportred to the atmosphere and the rest is decomposed or adsorbed to the solid phase. As a result, their concentration in the vadose zone has decreased significantly.

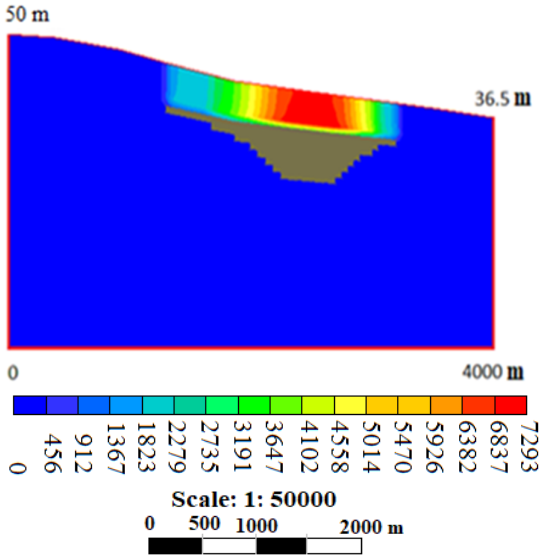

Figure 16. Two-dimensional simulation results: Distribution of gas-phase concentration (mg/l) of petroleum hydrocarbons for 36 years.

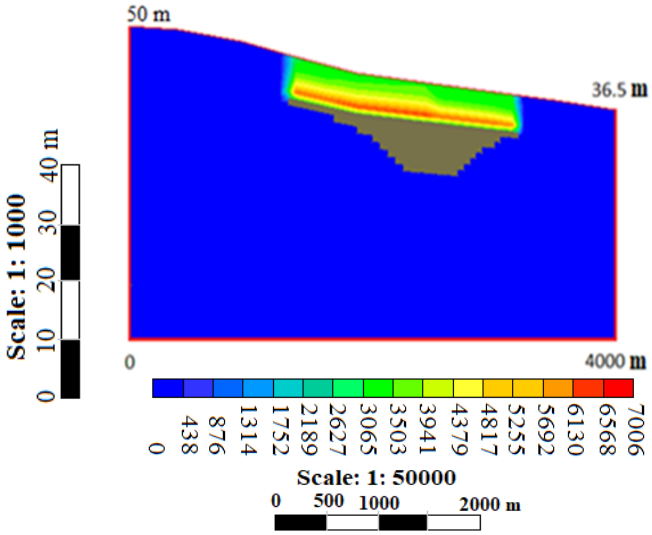

Figure 17. Two-dimensional simulation results: Distribution of gas-phase concentration (mg/l) of petroleum hydrocarbons for 50 years.

5.8. Scenario 8: Calculate the distribution of LNAPL in different phases

In this scenario, it is assumed that the free phase of LNAPL will remain on the groundwater-surface for up to 50 years and no remediation operations have been performed on it. With this assumption, the section of different phases is calculated. Figure (20) shows the time distribution of different phases. As the free LNAPL fraction decreases, the soluble and evaporated moieties increase. The absorbed phase fraction initially increases, but gradually decreases after about 11 years. This decrease is probably because a local equilibrium is established between the adsorbed phase and the soluble and gaseous phases. Figure (20) clearly shows that the process of evaporation into the atmosphere can significantly affect the evolution and transport of the free phase of LNAPL.

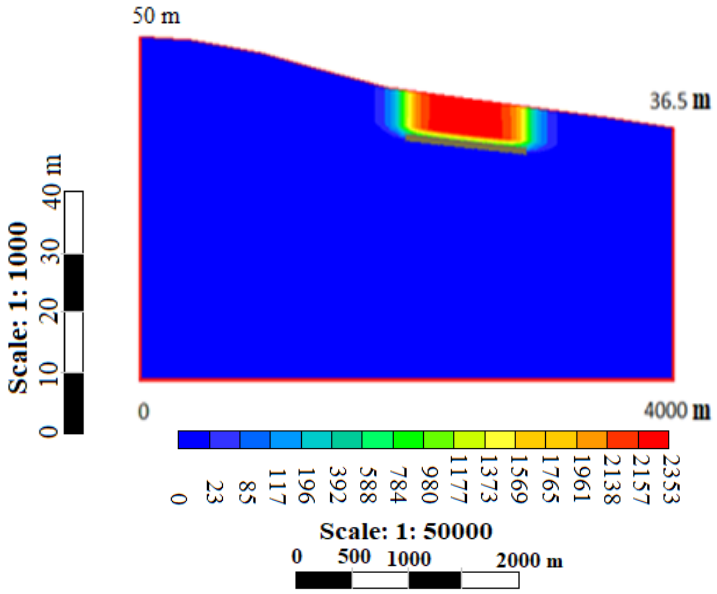

Figure 18. Two-dimensional simulation results: Distribution of gas-phase concentration (mg/l) for 50 years. In this scenario, a thin layer of the free phase of hydrocarbon pollutants remains on the surface of the groundwater aquifer after 50 years.

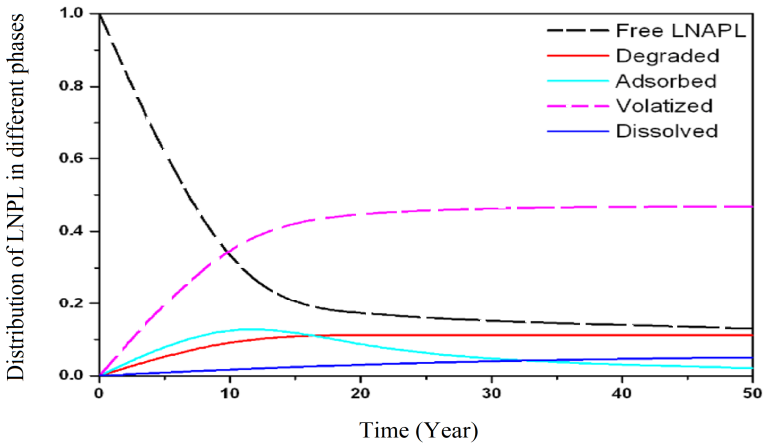

Figure 19. Distribution of LNAPL in different phases.

6. Conclusions

Modeling the transport of petroleum products in the groundwater flow system is important for the development of appropriate remediation systems. In this study, a numerical model was developed to simulate the movement of petroleum hydrocarbons in soil-gas and groundwater systems. This model takes into account the distribution of the residual LNAPL in soil, gas and liquid phases. The findings indicates that evaporation has a greater impact on LNAPL migration. The presence of the plume of

free-phase petroleum hydrocarbons and the geological features of the site played a role in the production and movement of the soluble plume.The majority of the spilled mass, even after 36 years since the leak, remained in the LNAPL free phase. The model presented in this paper has been able to accurately predict the thickness of the LNAPL column over groundwater. So that the finite volume numerical model predicted the maximum thickness of the LNAPL column between 7 and 7.5 meters at a distance of 2250 meters from the beginning of the investigated profile, which is in very good agreement with the field data.The prolonged migration of LNAPL results in groundwater pollution and represents a major source of soil contamination. As the first step to solve this environmental problem in the site of Tehran oil refinery and surrounding lands, the sources of pollution must be identified and removed. Then, the free oil over the ground water surface must be pumped and treated on the ground surface. This cleaning operation will take several years. However, it still cannot guarantee the complete removal of contamination from the site. The oil pollution can exist in two forms: dissolved in groundwater and between soil particles, in both forms acting as a continuous source of potential groundwater contamination. According to the conditions of the site, especially the presence of above-ground refining facilities and the need for their continuous operation, the proposed method applicable as the final phase of oil pollutant removal in Tehran oil refinery is the use of biological treatment. In the bioremediation method, the microbiological process is used to degrade or transform petroleum pollutants into less toxic or non-toxic compounds.

Acknowledgments

The Tehran Oil Refining Company, Iran, is gratefully acknowledged for their financial support. Additionally, the authors would like to express their gratitude to Shahrood University of Technology for the support of research.

Conflict of interest

The authors claim that they have no conflict of interest.

References

[1]. Mustafa, N., Mumford, K. G., Gerhard, J. I., O'Carroll, D. M., (2014). A three-dimensional numerical model for linking community-wide vapour risks, *Journal of Contaminant Hydrology*, *156*, 38-51.

[2]. Gupta, P. K., Yadav, B., and Yadav, B. K., (2019). Assessment of LNAPL in subsurface under fluctuating groundwater table using 2D sand tank experiments, *Journal of Environmental Engineering*, *145* (9), 04019048.

[3]. Gupta, P. K., and Yadav, B. K., (2020). Three-dimensional laboratory experiments on fate and transport of LNAPL under varying groundwater flow conditions, *Journal of Environmental Engineering*, *146* (4), 04020010.

[4]. Gupta, P. K., (2020). Pollution load on indian soil-water systems and associated health hazards: a review, *Journal of Environmental Engineering*, *146*(5), 03120004.

[5]. Gupta, P. K., (2020). Fate, transport, and bioremediation of biodiesel and blended biodiesel in subsurface environment: a review, *Journal of Environmental Engineering*, *146*(1):03119001.

[6]. Onwosi, C.O., Odibo, F.J.C., Enebechi, C.K., Nwankwegu, A.S., Ikele, A.I., Okeh, O.C., (2017). Bioremediation of diesel-contaminated soil by composting with locally generated bulking agents, *Soil and Sediment Contamination: An International Journal*, *26*, 438–456.

[7]. Kadri, T., Magdouli, S., Rouissi, T., Brar, S.K., (2018). Ex-situ biodegradation of petroleum hydrocarbons using Alcanivorax borkumensis enzymes, *Biochemical Engineering Journal*, *132*, 279–287.

[8]. Gupta, P. K., Yadav, B., Yadav, B. K., Sushkova, S., Basu, S., (2021). Engineered Bioremediation of NAPL Polluted Sites: Experimental and Simulation-Optimization Approach under Heterogeneous Moisture and Temperature Conditions, *Journal of Environmental Engineering*, *147*(8), 04021023.

[9]. Tran, H. T., Lin, C., Bui, X. T., Ngo, H. H., Cheruiyot, N. K., (2021). Aerobic composting remediation of petroleum hydrocarbon-contaminated soil. Current and future perspectives, *Science of the Total Environment*, *753*:142250.

[10]. Ugwoha, E., Amah, V. E., Agharese-ADU, P. E., (2021). Modelling the transport of crude oil in sandy soil, *International Journal of Chemistry and Chemical Engineering Systems*, http://www.iaras.org/iaras/journals/ijcces.

[11]. Margesin, R., Zimmerbauer, A., Schinner, F., (2000). Monitoring of bioremediation by soil biological activities. *Chemosphere*, *40*(4),339–346.

[12]. Farahani, M., Mahmoudi, D., (2018). Optimization, modeling and its conformity with the reality of physic-chemical and microbial processes of petroleum hydrocarbons reduction in siol: a case study of Tehran oil refinery, *Environmental Earth Sciences*, *77*, 329.

[13]. Kechavarzi, C., Soga, K., and Illangasekare, T. H., (2005). Two-dimensional laboratory simulation of

LNAPL infiltration and redistribution in the vadose zone, *Journal of Contaminant Hydrology*, *76* (3–4), 211–233.

[14]. Tomlinson, D. W., Rivett, M. O., Wealthall, G. P., and Sweeney, R. E., (2017). Understanding complex LNAPL sites: Illustrated handbook of LNAPL transport and fate in the subsurface, *Journal of Environmental Management*, *204* (Dec): 748–756.

[15]. Essaid, H. I., B. A. Bekins, and I. M. Cozzarelli., (2015). Organic contaminant transport and fate in the subsurface: Evolution of knowledge and understanding, *Water Resources Research*, *51* (7), 4861–4902.

[16]. Kacem, M., Esrael, D., Boeije, C. S., and Benadda, B., (2019). Multiphase flow model for NAPL infiltration in both the unsaturated and saturated zones, *Journal of Environmental Engineering*, *145* (11), 04019072.

[17]. Balint, A., (2021). Physical, chemical and toxicological properties of polycyclic aromatic hydrocarbons (PAHs) in human exposure assessments to contaminated soil and groundwater. *MATEC Web of Conferences 342*, 03016.

[18]. USEPA (2006). Edition of the Drinking Water Standards and Health Advisories. EPA/822/R0, p. 18.

[19]. Anderson, M. R., Johnson, R. L., Pankow, J. F., (1992). Dissolution of dense chlorinated solvents into ground water: dissolution from a well-defined residual source. *Groundwater 30*(2):250–256.

[20]. Soga, K., Page, J. W. E., Illangasekare, T. H., (2004). A review of NAPL source zone remediation efficiency and the mass flux approach, *Journal of Hazardous Materials*, *110*(1–3),13–27.

[21]. Yadav, B. K., and Hassanizadeh, S. M., (2011). An overview of biodegradation of LNAPLs in coastal (semi)-arid environment, *Water Air Soil Pollut. 220* (1–4): 225–239.

[22]. Das, D. B., Hassanizadeh, S. M., Rotter, B. E., and Ataie-Ashtiani, B., (2004). A numerical study of micro-heterogeneity effects on upscaled properties of two-phase flow in porous media, *Transport in Porous Media*, *56* (3): 329–350.

[23]. Das, D. B., and M. Mirzaei., (2012). Dynamic effects in capillary pressure relationships for two-phase flow in porous media: Experiments and numerical analyses, *AIChE Journal*, *58* (12): 3891–3903. https://doi.org/10.1002/aic.13777

[24]. Onaa, C., Olaobaju, E. A., Amro, M. M., (2021). Experimental and numerical assessment of light non-aqueous phase liquid (LNAPL) subsurface migration behavior in the vicinity of groundwater table, *Environmental Technology & Innovation*, *23*,101573.

[25]. Rivett, M.O., Wealthall, G.P., Dearden, R.A., McAlary, T.A., (2011). Review of unsaturated-zone transport and attenuation of volatile organic compound (VOC) plumes leached from shallow source zones, *Journal of Contaminant Hydrology*, *123* (3), 130e156.

[26]. Abreu, L. D. V., Ettinger, R., McAlary, T., (2009). Simulated soil vapor intrusion attenuation factors including biodegradation for petroleum hydrocarbons, *Groundwater Monitoring & Remediation*, *29* (1), 105-117.

[27]. Ng, G.H. C., Bekins, B. A., Cozzarelli, I. M., Baedecker, M. J., Bennett, P. C., Amos, R. T., (2014). A mass balance approach to investigating geochemical controls on secondary water quality impacts at a crude oil spill site near Bemidji, MN, *Journal of Contaminant Hydrology*, *164*, 1-15.

[28]. Ng, G.-H. C., Bekins, B. A., Cozzarelli, I. M., Baedecker, M. J., Bennett, P. C., Amos, R. T., Herkelrath, W. N., (2015). Reactive transport modeling of geochemical controls on secondary water quality impacts at a crude oil spill site near Bemidji, MN, *Water Resources Research*, *51* (6), 4156-4183.

[29]. Lang, D.A., Bastow, T.P., Van Aarssen, B.G.K., Warton, B., Davis, G.B., Johnston, C.D., (2009). Polar compounds from the dissolution of weathered diesel. *Groundwater Monitoring & Remediation*, *29* (4), 85-93.

[30]. Vasudevan, M., Johnston, C.D., Bastow, T.P., Lekmine, G., Rayner, J.L., Nambi, I.M., Kumar, G.S., Krishna, R.R., Davis, G.B., (2016). Effect of compositional heterogeneity on dissolution of non-ideal LNAPL mixtures, *Journal of Contaminant Hydrology*, *194*, 10-16.

[31]. Garg, S., Newell, C.J., Kulkarni, P.R., King, D.C., Adamson, D.T., Renno, M.I., Sale, T., (2017). Overview of natural source zone depletion: processes, controlling factors, and composition change, *Groundwater Monitoring & Remediation*, *37* (3), 62-81.

[32]. Lekmine, G., Sookhak Lari, K., Johnston, C.D., Bastow, T.P., Rayner, J.L., Davis, G.B., (2017). Evaluating the reliability of equilibrium dissolution assumption from residual gasoline in contact with water saturated sands, *Journal of Contaminant Hydrology*, *196*, 30-42.

[33]. Sookhak Lari, K., Davis, G.B., Johnston, C.D., (2016). Incorporating hysteresis in a multi-phase multi-component NAPL modelling framework; a multi-component LNAPL gasoline example, *Advances in Water Resources*, *96*, 190-201.

[34] Sookhak Lari, K., Rayner, J.L., Davis, G.B., (2018). Towards characterizing LNAPL remediation endpoints, *Journal of Environmental Management*, *224*, 97-105.

[35]. Yadav, B. K., Shrestha, S. R. and Hassanizadeh, S. M., (2012). Biodegradation of toluene under seasonal and diurnal fluctuations of soil-water temperature, *Water Air Soil Pollut. 223* (7): 3579–3588. https://doi.org /10.1007/s11270-011-1052-x.

[36]. Colombani, N., Mastrocicco, M., Prommer, H., Sbarbati, C., Petitta, M., (2015). Fate of arsenic, phosphate and ammonium plumes in a coastal aquifer affected by saltwater intrusion, *Journal of Contaminant Hydrology*, *179*: 116-131.

[37]. Liu, Y., Jiao, J. J., Luo, X., (2016). Effects of inland water level oscillation on groundwater dynamics and land-sourced solute transport in a coastal aquifer, *Coastal Engineering 114*, 347-360.

[38]. Teramoto, E.H.; Chang, H.K., (2019). Geochemical conceptual model of BTEX biodegradation in an iron-rich aquifer, *Applied Geochemistry*, 100, 293–304.

[39]. Powers, S. E., Abriola, L. M., and Weber Jr., W. J., (1994). An experimental investigation of NAPL dissolution in saturated subsurface systems: Transient mass transport rates, *Water Resources Research*, *30*, 321–332.

[40]. Lu, G., Clement, T. P., Zheng, C., Wiedemeier, T. H. (1999). Natural attenuation of BTEX compounds: model development and field-scale application, *Ground Water, 37*(5), 707-717.

[41]. Prommer, H., Barry, D. A., and Davis, G. B. (1999). A onedimensional reactive multi-component transport model for biodegradation of petroleum hydrocarbons in groundwater, *Environmental Modelling & Software*, *14*, 213–223.

[42]. Essaid, H. I., Cozzarelli, M. I., Eganhouse, P. R., Herkelrath, W. N., Belkins, B. A. and Delin, G. N., (2003). Inverse modeling of BTEX dissolution and biodegradation at the Bemidgi, M-N crude-oil spill site, *Journal of Contaminant Hydrology*, *67*, 269–299.

[43]. Atteia, O. and Guillot, C., (2007). Factors controlling BTEX and chlorinated solvents plume length under natural attenuation conditions, *Journal of Contaminant Hydrology*, *90*, 81–104.

[44]. Valsala, R. and Govindarajan, S. K., (2018). Interaction of dissolution, sorption and biodegradation on transport of BTEX in a saturated groundwater system: Numerical modeling and spatial moment analysis, *Journal of Earth System Science*,*127*:53.

[45]. Teramoto, E.H.; Chang, H.K., (2020). A screening model to predict entrapped LNAPL Depletion, *Water*, *12*, 334.

[46]. Gharedaghloo, B., Price, J. S., (2021). Assessing benzene and toluene adsorption with peat depth: Implications on their fate and transport, *Environmental Pollution*, *274*, 116477.

[47]. Zanello V., Scheger L. E., Lexow, C. (2021). Assessment of groundwater contamination risk by BTEX from residual fuel soil phase, *SN Applied Sciences*,*3*:307.

[48]. Pennell, K. G., Bozkurt, O., and Suuberg, E. M., (2009). Development and application of a three-dimensional finite element vapor intrusion model. *Journal of the Air & Waste Management Association*, *59* (4), 447–460.

[49]. Riis, C. E., Christensen, A. G., Mortensen, A. P., and Jannerup, H., (2010). Bioremediation of TCE in a fractured limestone aquifer using a novel horizontal passive biobarrier, Remediation: *The Journal of Environmental Cleanup Costs, Technologies & Techniques, 20* (2), 27–43.

[50]. Guo, Y., Holton, C., Luo, H., Dahlen, P., Gorder, K., Dettenmaier, E., and Johnson, P.C., (2015). Identification of alternative vapor intrusion pathways using controlled pressure testing, soil-gas monitoring, and screening model calculations, *Environmental Science & Technology*, *49*, 13472–13482.

[51]. Shirazi, E., and Pennell, K.G., (2017). Three-Dimensional Vapor Intrusion Modeling Approach that Combines Wind and Stack Effects on Indoor, Atmospheric, and Subsurface Domains. *Environmental Science: Processes & Impacts 19*, no. 12: 1594–1607.

[52]. McHugh, T., and L. Beckley., (2018). Sewers and Utility Tunnels as Preferential Pathways for Volatile Organic Compound Migration into Buildings: Risk Factors and Investigation Protocol, Fort Belvoir, Virginia: Defense Technical Information Center.

[53]. Roghani, M., Jacobs, O.P., Miller, A., Willett, E. J., Jacobs, J. A., Viteri, C. R., Shirazi, E., and Pennell, K. G., (2018). Occurrence of chlorinated volatile organic compounds (VOCs) in a sanitary sewer system: Implications for assessing vapor intrusion alternative pathways, *Science of The Total Environment*, *616*, 1149–1162.

[54]. Shirazi, E., Hawk, G. S., Holton, C. W., Stromberg, A. J., and Pennell, K. G., (2020). Comparison of modeled and measured indoor air trichloroethene (TCE) concentrations at a vapor intrusion site: Influence of wind, temperature, and building characteristics, *Environmental Science: Processes & Impacts*, *22* (3), 802–811.

[55]. Roghani, M., Li, Y., Rezaei, N., Robinson, A., (2021). Modeling Fate and Transport of Volatile Organic Compounds (VOCs) Inside Sewer Systems, *Groundwater Monitoring & Remediation*, *41*(2),112–121.

[56]. Volkman, J.K., Alexander, R., Kagi, R.I., Rowland, S.J., Sheppard, P.N., (1984). Biodegradation of aromatic hydrocarbons in crude oils from the Barrow Sub-basin of Western Australia, *Organic Geochemistry*, *6*, 619-632.

[57]. Peters, K. E., Moldowan, J. M., (1993). The Biomarker Guide: Interpreting Molecular Fossils in Petroleum and Ancient Sediments. Prentice Hall, Englewood Cliffs, NJ, USA.

[58]. Christensen, L. B., Larsen, T. H., (1993). Method for Determining the Age of Diesel Oil Spills in the Soil,

Groundwater Monitoring & Remediation, *13* (4): 142-149.

[59]. Blanc, P.C.D., McKinney, D.C., Speitel, G.E., (1996). In: Corapcioglu, M.Y. (Ed.), Advances in Porous Media. Elsevier, Austin, USA, pp. 1-86.

[60]. Gaylord, J., (1998). Remediation of petroleum contaminated soils: biological, physical, and chemical processes. CRC press.

[61]. Prommer, H., Davis, G.B., Barry, D.A., (1999). Geochemical changes during biodegradation of petroleum hydrocarbons: field investigations and biogeochemical modelling, *Organic Geochemistry*, *30* (6), 423-435.

[62]. Prommer, H., Barry, D.A., Davis, G.B., (2002). Modelling of physical and reactive processes during biodegradation of a hydrocarbon plume under transient groundwater flow conditions, *The 2000 Contaminated Site Remediation Conference: From Source Zones to Ecosystems, 59* (1), 113-131.

[63]. Agah, A., Doulati Ardejani, F. and Ghoreishi, H., (2011). Two-dimensional numerical finite volume modeling of processes controlling distribution and natural attenuation of BTX in the saturated zone of a simulated semi-confined aquifer. *Arabian Journal Geoscience*.

[64]. Agah, A., Doulati Ardejani, F. and Ghoreishi, H., (2012). An Assessment of Factors Affecting Reactive Transport of Biodegradable BTEX in an Unconfined Aquifer System, Tehran Oil Refinery, Iran. *International Journal of Mining and Geo-Engineering (IJMGE)*, *46* (2), 193-208.

[65]. Blagodatsky, S., Smith, P., (2012). Soil physics meets soil biology: towards better mechanistic prediction of greenhouse gas emissions from soil. *Soil Biology and Biochemistry*, *47*, 78-92.

[66]. Miller, C.T., Dawson, C.N., Farthing, M.W., Hou, T.Y., Huang, J., Kees, C.E., Kelley, C.T., Langtangen, H.P., (2013). Numerical simulation of water resources problems: models, methods, and trends, *Advances in Water Resources* ,*51*, 405-437.

[67]. Agah, A., and Doulati Ardejani, F., (2015). A CFD Model for Prediction of the Role of Biomass Growth and Decay on the Aerobic Biodegradation of BTEX fate and Transport in an Unconfined Aquifer System, *International Journal of Environmental Research*, *9*(3),933-942.

[68]. Hidalgo, K. J., Sierra-Garcia, I. N., Dellagnezze, B. M.,de Oliveira, V. M., (2020). Metagenomic Insights Into the Mechanisms for Biodegradation of Polycyclic Aromatic Hydrocarbons in the Oil Supply Chain, *Frontiers in Microbiology*, *11*, 561506.

[69]. Parker, J.C., (2003). Modeling volatile chemical transport, biodecay, and emission to indoor air, *Groundwater Monitoring & Remediation*, *23* (1), 107-120.

[70]. Knight, J. H., Davis, G. B., (2013). A conservative vapour intrusion screening model of oxygen-limited hydrocarbon vapour biodegradation accounting for building footprint size, *Journal of Contaminant Hydrology*, *155*, 46-54.

[71]. Akbariyeh, S., Patterson, B. M., Kumar, M., Li, Y., (2016). Quantification of Vapor Intrusion Pathways: An Integration of Modeling and Site Characterization, *Vadose Zone Journal*. *15* (10).

[72]. Membere, E., Johnson, E., (2019). Diffusive-Gas Transport of Volatile Organic Carbons from a Source in an Unsaturated (Vadose) Zone, *IOSR Journal of Environmental Science, Toxicology and Food Technology (IOSR-JESTFT)*, 13(1),11-18.

[73]. Kim J. and Corapcioglu M. Y., (2003). Modeling dissolution and volatilization of LNAPL sources migrating on the groundwater table, *Journal of Contaminant Hydrology*, *65*, 137-158.

[74]. Spalding, D. B., (1981). A general purpose computer program for multidimensional one- and two-phase flow, *Mathematics and Computers in Simulation*, *23*(3):267–276.

[75]. Doulati Ardejani, F., Singh, R. N., Baafi, E. Y., (2004). Use of PHOENICS for solving one dimensional mine pollution problems. PHOENICS Journal of Computational Fluid Dynamics and its Applications, *16*,23.

[76]. Doulati Ardejani, F., Jannesar Malakooti, S., Shafaei, S.Z., Shahhosseini, M., (2014). A numerical multi-component reactive model for pyrite oxidation and pollutant transportation in a pyrite-bearing, carbonate-rich coal waste pile, Anjir Tangeh, northern Iran, *Mine Water and the Environmen*t, *33*, 121-132.

[77]. www.ngdir.ir

[78]. FusioneTechno Solutions Co. (2006).

[79]. Han, K., Levenspiel, O., (1988). Extended Monod kinetics for substrate, product and cell inhibition, *Biotechnology & Bioengineering*, *32*, 430 – 437.

[80]. Okpokwasili G. C, and Nweke C. O., (2005). Microbial growth and substrate utilization kinetics, *African Journal of Biotechnology*, *5*(4), 305-317.

[81]. Sanders, P., (2002). Microbial degradation kinetics of volatile organic hydrocarbons: effect of BTEX concentration and environment, Technical report, 1-91.

مدل‌سازی انتقال راکتیو چند فازی هیدروکربن‌های نفتی در منطقه صنعتی ری

آزاده آگاه[1*] و فرامرز دولتی ارده جانی[2]

۱- گروه مهندسی معدن، دانشکده مهندسی شهید نیکبخت، دانشگاه سیستان و بلوچستان،زاهدان، ایران
۲- دانشکده معدن، دانشگاه تهران، تهران، ایران

ارسال ۲۰۲۴/۰۱/۱۹، پذیرش ۲۰۲۴/۱۰/۳۰

* نویسنده مسئول مکاتبات: agah_eng@eng.usb.ac.ir

چکیده:

هدف این مطالعه ایجاد مدلی برای نشان دادن مهاجرت هیدروکربن‌های نفتی که به دلیل نشت از مخازن ذخیره‌سازی واقع در زیر سطح به محیط زیرزمینی نفوذ می‌کنند، می باشد. مدل انتقال مایعات فاز غیرآبی با مدل‌های انتقال آلاینده در دو بعد برای پیش‌بینی آلودگی آب های زیرزمینی و خاک-گاز ناشی از مهاجرت مایعات فاز غیرآبی سبک روی سطح آب ادغام شد. برای به دست آوردن جواب های عددی از روش حجم محدود استفاده شد. یافته ها نشان داد که تبخیر به طور قابل توجهی بر مهاجرت مایعات فاز غیر آبی تأثیر می گذارد. تولید و حرکت ستون محلول تحت تأثیر ویژگی های زمین شناسی مکان و وجود ستون فاز آزاد قرار گرفت. مقایسه پیش‌بینی‌های مدل و نتایج حاصل از مطالعات میدانی برای ضخامت ستون مایعات فاز غیرآبی روی آب نشان‌دهنده تطابق خوب بین نتایج دو روش با میانگین خطای کمتر از ۵ درصد است. حداکثر ضخامت ستون مایعات فاز غیرآبی بین ۷ تا ۷.۵ متر در فاصله ۲۲۵۰ متری از ابتدای پروفیل مورد بررسی به دست آمد. اگرچه ۳۶ سال از وقوع نشت می گذرد، اما مقدار قابل توجهی از جرم ریخته شده هنوز در مایعات فاز غیرآبی باقی مانده است. مهاجرت طولانی مدت مایعات فاز غیرآبی در این بازه زمانی منجر به آلودگی آب های زیرزمینی و تجمع مقادیر قابل توجهی خاک آلوده شده است.

کلمات کلیدی: مدل دو بعدی، انتقال راکتیو چند فازی، مایعات فاز غیرآبی، آب زیرزمینی، منطقه صنعتی ری.